IOP Conf. Series: Earth and Environmental Science 1078 (2022) 012048 doi:10.1088/1755-1315/1078/1/012048

Plus minus zero: carbon dioxide emissions of plus energy buildings in operation under consideration of hourly German carbon dioxide emission factors for past, present and future

A Studniorz [1], D Wolf [3], N Kiessling [3], R Fahrich [2], C Banhardt [3] and G Tsatsaronis [1]

[1] Technische Universität Berlin, Chair of Energy Engineering and Environmental Protection, Marchstraße 18, 10587 Berlin

[2] Technische Universität Berlin, Hermann-Rietschel-Institut, Marchstr. 4, 10587 Berlin

[3] HPS home power solutions, Carl-Scheele-Straße 16, 12489 Berlin

E-mail: alex.studniorz@tu-berlin.de

Abstract. The energy supply of private household buildings accounted for 16 % of the total German CO_2-emission in 2020. To fulfil the targets of a climate neutral building sector in 2045, both, energy efficiency as well as on-site use of Renewable Energies in buildings are needed. One concept of a climate neutral building is the so-called Efficiency House Plus, that features large photovoltaic systems making it seemingly energy self-sufficient and CO_2-negative by feeding in more electric energy into the grid than needed for its operation on a yearly basis. In fact, houses of this type are highly grid dependent especially during winter months due to their solely electrically based energy supply and a missing long term energy storage. This paper analyses the CO_2 -emission of Energy Efficiency Plus houses more in detail on a timely resolved basis for the German electric supply system of the year 2013, 2021 and a perspective one 2030. An alternative calculation approach for simplified normative evaluation of such buildings is proposed.

Keywords: single family house, CO_2 sustainability assessment, energy exchange, dynamic building simulation, energy system analysis

1. Introduction

The climate protection target made within the Paris Agreement [1] to limit the increase in the global average temperature possibly below two degrees Celsius and, if possible, to 1.5 degrees Celsius, above the pre-industrial level were the basis of the Federal Climate Change Act [2]. This so-called “Bundesklimaschutzgesetz” (KSG) was revised in 2021 [3] This reduction goal is targeting the emissions during the operation of buildings, which makes sence regarding the building stock where operation energy is the main GHG emission contributor. However, a recent study [4] with an analysis of more than 650 building life cycle assessment (LCA) results show that the so-called embodied greenhouse gas (GHG) emissions are more and more dominating the life cycle of new buildings. Embodied emissions stand for the emission of manufacturing and processing of building materials. Thus it becomes obvious, that the whole life cycle of buildings

needs to be analyzed to assure their climate neutrality. Since embodied GHG emissions are unavoidable, the decision whether a building is climate neutral or not, depends on the (negative) GHG emissions during operation.
One building concept that seemingly achieves a CO_2 negative operation is the so-called "Effizienzhaus Plus" (Efficiency House Plus (EHP)) [5]. EHPs feature large photovoltaic (PV) systems, offering an annual amount of electric energy that exceeds the electric and heating energy demand within a year. The remaining surplus of PV energy is fed into the electric grid. The assumption regarding this exported PV energy is, that it substitutes grid electricity and its corresponding CO_2 emission. While the approach is straighforward, the central question arises about the *corresponding* CO_2 emissions of the grid electricity being substituted by the exported PV energy.
In the absence of a detailed data basis, most CO_2 calculations apply a uniform and constant CO_2 emission factor to account for both, electric energy drawn from and fed into the electric grid, although recent studies [6, 7, 8] show that this approach can distort the actual proportion of CO_2 emission and CO_2 relief of energy exchange between buidlings and the electric grid.
This paper reviews the influence on the CO_2 emission calculation in operation of EHPs when using hourly CO_2 emission factors of the electric grid in comparison to the common static approach.

2. Background and Method

To understand how EHPs reach a negative CO_2 emission in operation it is essential to clarify their general working principle as well as the way of how energy and CO_2 balances are applied. After that the dynamic CO_2 emissions of grid electricity in Germany are analysed, representing one part to reveal the net CO_2 emissions of EHP. The last part needed to achieve this goal is a rigorous building simulation model offering reliable data on how the grid usage of EHPs evolves throughout a year.

2.1. Efficiency Plus Buildings and their CO_2 emission rating

As per definition EHPs reach negative values of primary and final energy demand. EHPs offer low space heating demand that is supplied most of the times by heat pumps. In addition, they contain a large PV system, that generates more electrical energy per year than needed for electricity and heating requirements. This setup is favourable in general, since more PV capacity and sector coupling is needed to enhance the energy transition in Germany.
However, energy supply and demand are not always such that a direct supply can be achieved solely by the local PV system at all times. First EHPs reached temporal shares of 30-50 % in which the energy demand was supplied by the PV-System only, whereas latest example show values of up to 70-80 % incorporating batteries as short-term energy storages.
Thus, EHPs are fundamentally grid dependent due to two reasons. On the one hand, to achieve reliable energy supply for the remaining part of a year, on the other hand to be able to make use of the PV surplus energy by feeding it into the electric grid. From this point of view it becomes clear that the 'plus' in energy of EHPs is time dependent. While during summer they produce an energy surplus, EHPs strongly rely on grid electricity in winter times.
The approach used in [5] to estimate the CO_2 emissions of EHPs follows DIN 18599-1, so that CO_2 emissions of imported from and exported to the grid energy can be summed up into one net CO_2 emission. The DIN 18599-1 allows the same equations for CO_2 emission calculation as for the primary and final energy demand calculation. As concrete values for accounting CO_2 emissions of both, electricity drawn from and fed into the electric grid, a CO_2 emission factor of 550 $^{g\,CO_2}/_{kWh}$ is given, representing the annual average value of electricity within the German electric grid in 2014. With an average specific PV energy surplus of 20 $^{kWh}/_{m^2 \cdot a}$ and following the declaration of 550 $^{g\,CO_2}/_{kWh}$ as the constant CO_2 emission factor, EHPs save 12 $^{kg\,CO_2}/_{m^2 \cdot a}$.

2.2. Hourly based CO_2 *emission factor of the German electricity mix*

The actual German power plant system covers the national electricity demand under constantly changing operation of fossil and renewable energy sources. Hourly data on power plant operation are available in several publicly accessible databases (e.g. Fraunhofer ISE Energy-Charts, Agorameter). Technology-specific CO_2 emission factors (e.g. [9]), as shown in **Table 1**, allow the absolute emissions of the German power plant system to be calculated from the hourly-resolved power plant input, as well as a specific CO_2 emission factor of the current electricity mix based on the electricity demand covered. The CO_2 emission factor can be used to characterize the CO_2 intensity of electricity production in the face of fluctuating electricity demand. This hourly CO_2 emission factor is shown for the years 2013 and 2021 and a future scenario 2030 in **Figure 1 (a)**. The diagram in **Figure 1 (b)** contains the same data points but shown as a carpet plot to better illustrate daily and weekly changes of the CO_2 emission factor. High and low values of the CO_2 emission factor can be assigned using the adjacent colorbar.
Clearly recognizable is the 'photovoltaic ellipse' with the main axis February-October and minor axis 08:00-16:00 at the end of June. Likewise, isolated vertical yellowish and green bars ('wind turbine towers') can be recognized mainly in March and May, which are caused by constant highwind power feed in times lasting for days. Nevertheless, it must be noted that in summer nights with little wind, the CO_2 emission factor reaches high values, because almost all electricity demand must be covered by fossil energy sources. And finally fossil power plant supply big shares of the electric energy demand during November, December and January. Within **Figure 1 (a)**

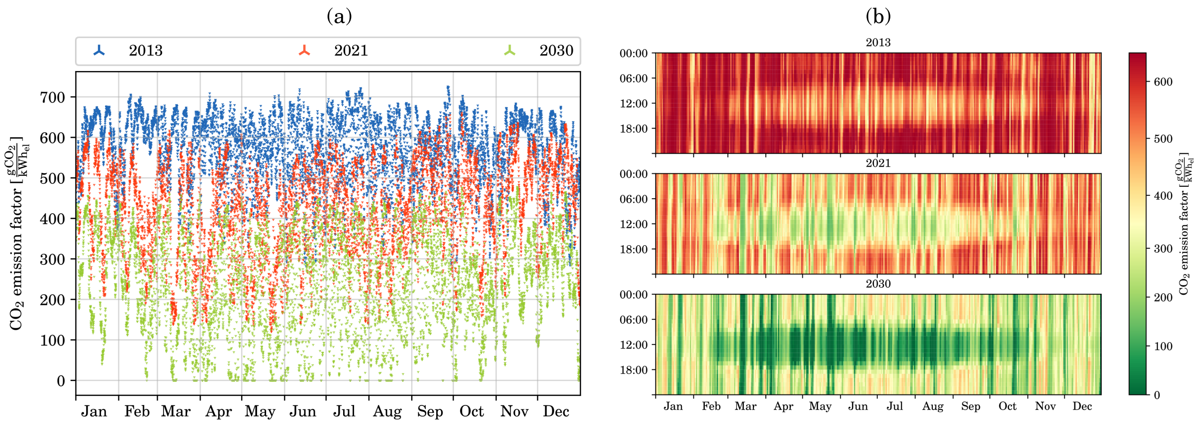

Figure 1. Hourly based CO_2 emission factor of the German power plant system for the years 2013, 2021 and extrapolated scenario 2030; with data from Agorameter

two phenomena can be described. On the one hand, the average level of the CO_2 emission factor continues to decrease from 2013 (Ø 573 $g\,CO_2/kWh$) through the year 2021 (Ø 422 $g\,CO_2/kWh$) to the future scenario 2030 (Ø 233 $g\,CO_2/kWh$). On the other hand, the range of values of the CO_2 emission factor increases from 2013 to 2021/2030. Both phenomena can be explained by the growing share of renewable energies. In 2013, the share of renewables in electricity generation was about 10 %, while in 2021 it was already 42 % and is assumed to be 68 % in the 2030 future scenario [10]. With an increasing share of renewable energies, specific CO_2 emissions decrease as fossil power plants are used less. On the other hand, the range of values of the CO_2 emission factor increases, since renewable energies no longer only support the electricity supply in an additive manner (2013), but take over relevant shares (in 2021) or even completely (in 2030), whereby alternating large shares of renewable and fossil power plants are used and explain the large differences in the CO_2 emission factor. Thus, in 2021, there were times when

Table 1. CO_2 emission factors and shares of fossil power plant types for the future scenario 2030

Power plant type	CO_2 emission $\mathrm{t\,CO_2/MWh}$	Cap (GW)	Share(%)
Gas	0.37	40.5	80
Coal	1.09	3	6
Lignite	0.82	3	6
Others	1.50	4	8
Fossil power plant system 2030	0.53	50.5	100

the electricity demand was still almost exclusively covered by fossil fuels (ca. 600 $\mathrm{g\,CO_2/kWh}$) and times when a CO_2 emission factor of only 150 $\mathrm{g\,CO_2/kWh}$ could be achieved with the help of renewable energy, which was not possible in 2013. For 2030, the CO_2 emission factor drops to a value of 0 $\mathrm{g\,CO_2/kWh}$ at some times when all electricity demand is met by renewables. If the supply of renewable energies is insufficient, the residual load in 2030 will still be covered by a backup system consisting of conventional power plants. The supposed composition of this backup capacity follows [10] and is shown in **Table 1**. Based on this breakdown, a weighted emission factor for the backup power plants was determined (0.53 $\mathrm{t\,CO_2/MWh}$).

2.3. Minute based heat and electricity supply of a single-family house

The linking element missing to utilize the hourly based CO_2 emission factors to calculate more appropriate net CO_2 emissions is a precise, consistent, and reliable knowledge about the timely resolved electric power demand of a single family house. This can be achieved by a rigorous building model offering a minute-by-minute resolved thermal and electrical energy demand and supply simulation of an EHP including energy exchange with the electric grid. In the following the developed model named "piceaSim" including the energy system setup, namely models of PV, inverter, battery, heat pump, thermal storage, underfloor heating system, and finally the building model will be described briefly. Furthermore, model reliability is proven by a cross validation for the building model with two other simulation software.

Modelling and simulation of piceaSim was performed in MATLAB/Simulink. PVLib [11] was used to calculate incident surface radiation and power output, extended by a thermal time constant model to reflect the module's transient cell temperatures [12, 13] . Validation with the commercially available software PV*SOL proved high accuracy at minutely resolution, resulting in a coefficient of determination $R2 = 0.99$. Conversion efficiency curves for PV-to-battery, PV-to-load and battery-to-load of a current domestic hybrid inverter were obtained from a series of laboratory measurements. The battery state of charge model applied ampere counting method considering dynamic charge-acceptance. The battery voltage was determined through a 2-D lookup table derived from laboratory measurements. The heat pump was modelled following a widely adopted performance map (e.g. manufacturers EN 14511 European standard test data) based grey box approach including a lumped parameter thermal mass to account for non-stationary behaviour such as cycling losses resulting from condenser or evaporator heat up and cool down [14, 15]. Validation of these equation-fit models has been carried out in numerous studies proving their well-suitedness for building energy simulations [16, 17]. The stratified thermal energy storage is divided into two sections: The top part supplying domestic hot water through an external heat exchanger (central freshwater station), the bottom part acting as a buffer and hydraulic separator for the underfloor heating system. An adaptation of [18] using the buoyancy algorithm from [19] was implemented, a description of the freshwater station model

can be found in [20]. The hydronic layout represents a common scheme for modern single-family homes [21, 22, 23]. Heat pump and tank were sized according to European standard EN 15450 and recommendations of the national heat pump association [24]. The 5R1C model proposed by ISO 13790 was extended for a second thermal capacitance comprising air mass. In addition, underfloor heating slabs were discretized more detailed as an electrical analogy ("Beuken" model) [25] and coupled to the building zone following an approach presented and validated in [26, 27, 28]. Heat delivery from carrier medium was reduced from a 3 dimensional to simplified 1 dimensional heat flow [29, 30, 31].The efficiency of ventilation heat recovery was calculated utilizing the NTU method [32]. Measured historical weather datasets for the city of Potsdam in 10-minute resolution were acquired from DWD. Generation of minutely load profiles considering season, weekday and cloud amount for household electricity and domestic hot water demand was performed for each weather dataset according to national guideline VDI 4655:2021.
The 5R2C building model in MATLAB as part of piceaSim was cross validated with other existing simulation models to ensure its prediction quality for the building heat demand. For validation, the architectural design of a prototype single-family house was used and three building models were implemented in MATLAB (piceaSim), Modelica (BuildingsLibrary) and the industry simulation software IDA ICE for comparison. The models implemented in piceaSim and Modelica were single zone building models, while the IDA ICE model was implemented as a multizonal model to assess comparability for the single zone model to multizonal building behaviour. All parameters of the three building models were harmonized including the dimensions of outer walls, windows, floors and roof, as well as the thermal properties of the corresponding building components. For simulation the same weather and solar radiation data (TRY 2015) were chosen, and air infiltration rates, air handling units, thermal bridge corrections and internal heat gains were aligned. The resulting monthly heat demands are shown in **Figure 2 (b)**. The

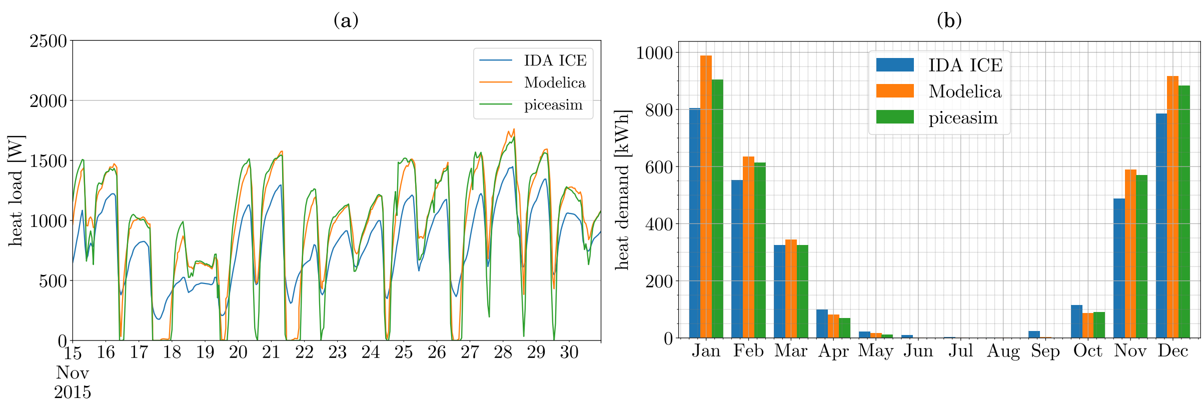

Figure 2. Cross validation of three building models by: (a) dynamic building heat load shown for November; (b) monthly heat demand (both based on climate data time series TRY 2015)

calculated monthly heat demand for the piceaSim building model is comparable to the results of the examined Modelica and IDA ICE models. The monthly result positions itself right between the results of the other two models for the winter months. The cumulated yearly heat demand results in 3228 kWh_{th} for IDA ICE, 3664 kWh_{th} for Modelica and 3464 kWh_{th} for piceasim. For the dynamic heat demand simulation, the piceaSim and Modelica models provide very similar results over the whole year. In **Figure 2 (a)** the simulated building heat demand for all three models is shown for the second half of November as an example. Since the IDA ICE model is implemented as a multizonal model, heat demand is dampened due to the heat exchange between rooms and added heat storage in partition walls. Another difference is the minimum heating

demand. Rooms with limited exposure to solar gains need to be heated in the multizonal model, while the single zone models applies solar gains to the whole building volume, dropping the heat demand to zero for the times solar gains overtake heat demand.
The results for the dynamic behaviour and monthly aggregated results for heat demand suggest that the building simulation model in piceaSim provides very similar results compared to the simulation models from Modelica. The single zone models perform similarly in monthly heat demand simulation and dynamic behaviour. The results are comparable to industry simulation software IDA ICE, although the heat demand of the multizonal model tends to be lower and shows a behaviour for certain zones that are not represented in the single zone models. Still the single zone model of piceaSim allows simulation within reasonable error ranges to estimate the building heat demand. The building model used within in the simulations of this contribution has a specific head demand of 38 $kWh_{th}/m^2 \cdot a$.

3. Simulation

EPHs can be characterized by their average electricity surplus of around 20 $kWh_{el}/m^2 \cdot a$ [5]. Taking this average value into account a parameter study with PV-capacities varying between 8/10/12/14/16 kW_{peak} (180° azimuth – South, tilt angle 30°) and an annual household electricity demand of 2500/3000/3500 kWh_{el} still without thermal supply was perfomed to cover a wider range of possible system setups including the one with an electricity surplus of around 20 $kWh/m^2 \cdot a$. Furthermore, all combinations mentioned were simulated for an EPH with and without a battery as well as for the two weather data time series of 2013 and 2021 (weather data time series of future-scenario 2030 equals 2021).
The simulated system behaviour ist presented in **Figure 3 (a)** for three days of summer and in **Figure 3 (b)** for winter. It can be seen, that during summer almost no grid demand is existent, although the household load is high. Due to high PV gains all electric demands are supplied and in addition large amounts of PV surplus energy can be fed into the grid. This is different in winter, where only small PV gains can be achieved and an additional heating demand must be supplied. This leads to almost continuous need for grid power supply. For the same time sections chosen to illustrate the system behaviour the timely varying CO_2 emission factor is shown in **Figure 3 (c)** for summer and **Figure 3 (d)** for winter respectively. On basis of these simulations the interconnection between times of grid demand (blue) and feed-in (yellow) to the dynamic CO_2 emission factor are evaluated precisely throughout the year.
As shown exemplarily in **Figure 3** the grid demand takes place in time sections of high CO_2 emission factors whereas feed-in mostly takes place during times of low CO_2 emission factors. To characterize a system setup, an average value of the CO_2 emission factor was calculated for grid demand and feed-in considering the actual CO_2 emission factor weighted by the amount of energy drawn from or supplied to the electric grid throughout the year. The results of all system setups simulated will be shown in the following.

4. Results

Simulations were performed for multiple combinations by varying the four parameters of installed PV-capacity, electricity demand, availability of a battery as well as different datasets for weather and CO_2emission factor. As a representative case the results of 12 kW_{peak} PV and 3500 kWh_{el} household electricity demand are selected and will be shown grouped by the three weather- and CO_2-datasets used and the two scenarios of EHP with (PV + battery) and without battery (PVOnly). Simulation results of all other scenarios are represented by an additional range of values illustrated by spread bars around the representative case. The presentation of results can be divided into relative and absolute key indicators. As the central relative value, the weighted average CO_2 emission factor was calculated for times of grid use and feed-in times. As absolute

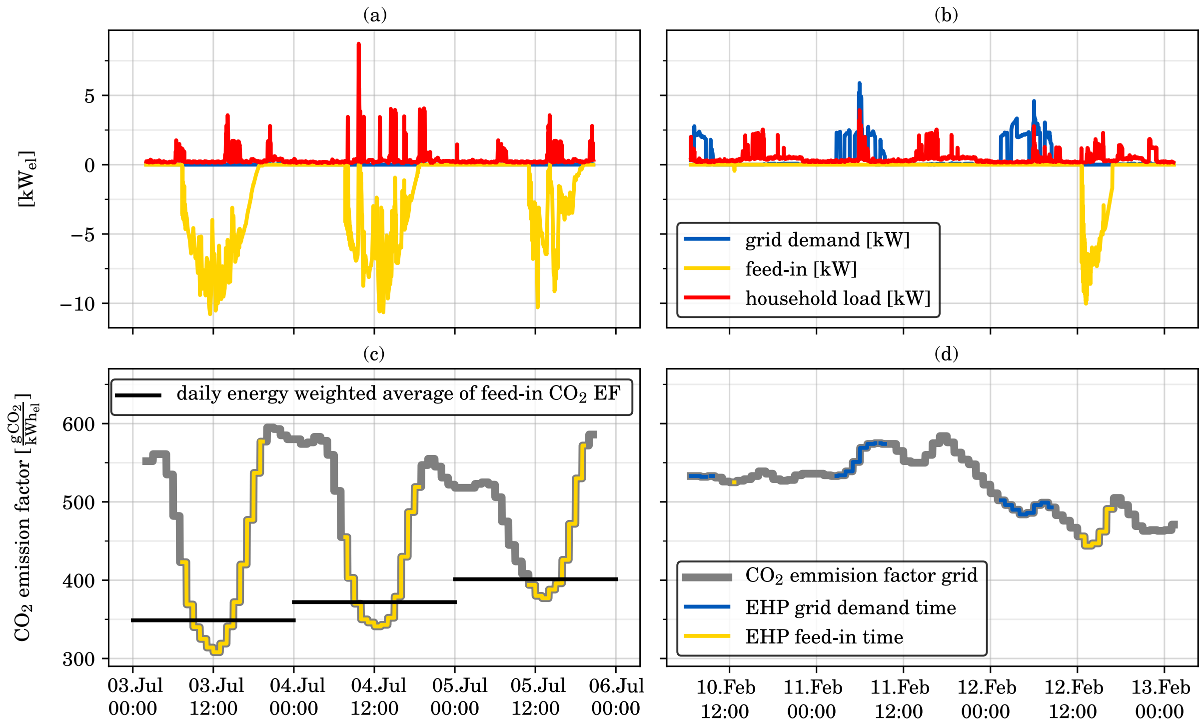

Figure 3. Simulated EHP system behaviour and timely interlinked CO_2 emission factors for (a,c) 3 days of summer and (b,d) 3 days of winter (EHP - PVBat - 12 kW_{peak} PV - 3500 kWh_{el} electricity demand) - 11 kWh_{inst} battery

values of CO_2 emission for grid use and feed-in were calculated to estimate the net CO_2 emission. The relation between the CO_2 emission factor for grid use and feed-in times for the three reviewed datasets 2013, 2021 and 2030 is shown in **Figure 4** for EHPs with and without battery.

It has to be emphasized that for both scenarios, PVOnly and PV + battery identical weather

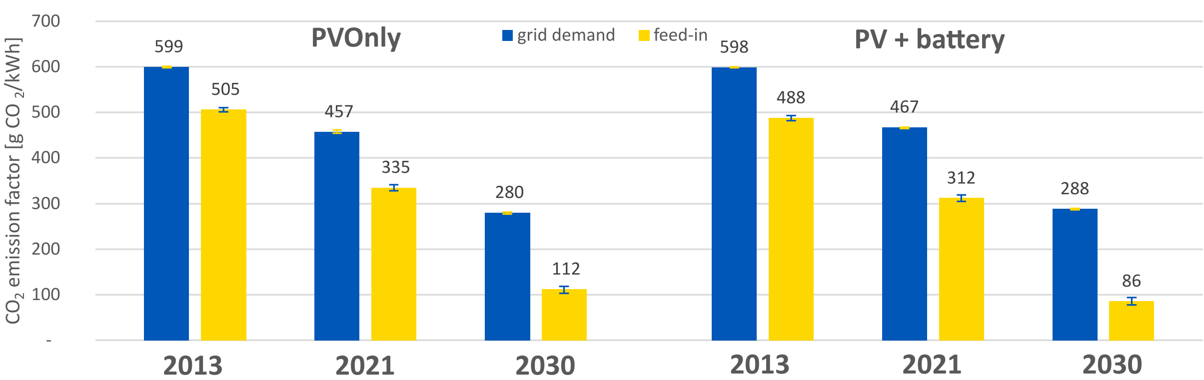

Figure 4. Weighted average CO_2 emission factor calculated by dynamic simulation for grid demand and feed-in times of EPH without (PVOnly) and with battery (PV+battery) for different years

and CO_2 emission time series data is used.

Two main trends can be observed in both setups with and without battery. Firstly, a growing

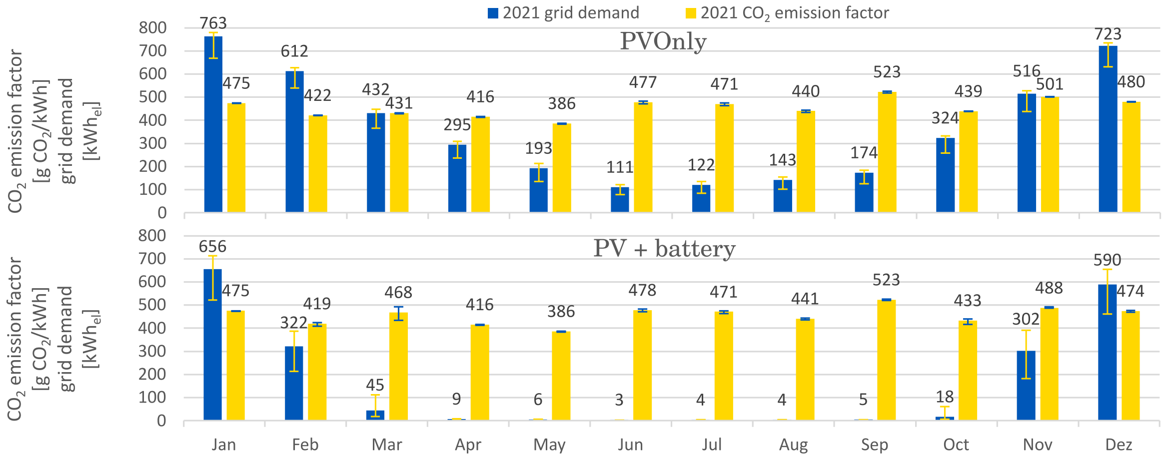

Figure 5. Comparison of monthly electricity demand and CO_2 emission factor for variation of PV capacity for EHP without and with battery show almost constant CO_2 emission factor for electricity drawn form the grid in 2030

gap between the CO_2 emission factor of grid demand and feed-in times is clearly visible. The difference accounts for scenario without/with battery up to 94/110 $^{g\,CO_2}/_{kWh_{el}}$ in 2013, 122/155 $^{g\,CO_2}/_{kWh_{el}}$ in 2021 and 168/202 $^{g\,CO_2}/_{kWh_{el}}$ in 2030. Moreover, the level of CO_2 emission factor for both, grid use and feed-in, decreases over the years due to the decarbonization of the electricity sector. To be highlighted is the only minor deviation of the simulated system configurations regarding the relative CO_2 emission factors of EHPs with and without battery.

The central finding is, that the CO_2 emission factor of energy drawn from the grid is almost equal throughout the year, implying a comparable share of fossil power plants in the grid during summer nighttime and winter season (an insight matching **Figure 1 (b)**). Nevertheless, it can be seen, that grid use mainly occurs during the winter months (1,2,11,12). The share of grid power demand within these four months accounts up to 58-60 % for EHPs without and to 91-96 % for EHPs with battery. EHPs with battery show lower grid use in summer months whereas grid use during winter remains high.

The results of using the static method (DIN 18599) in comparison to the dynamic method (introduced here) to account for the net CO_2 emissions of EHPs are presented in **Figure 6**. Here, the absolute net CO_2 emissions in operation, calculated by the two different methods, are presented in absolute numbers [kg CO_2 per year] for the datasets 2013, 2021 and 2030 for EHP with and without battery. Negative values represent a relief of the global climate. Regarding the static method (red bars) negative values are achieved by any EHP in every year. In contrast, CO_2-savings calculated with the dynamic method (green bars) reach significant lower values throughout all datasets and system configurations simulated.

A remarkable deviation between the two methods appears within the datasets of 2030, where net CO_2 emissions of EHP turn positive for some setups mirroring a net CO_2 emission despite a surplus of PV energy supplied to the electric grid. This finding is in line with the increasing gap of specific CO_2 emission over the years from 2012 to 2030 (compare **Figure 4**).

The spread bars shown in **Figure 6** indicate the values of different system setups and illustrate the strong influence of the PV-capacity and electricity demand on the results. All simulated system setups shown reached a PV energy surplus which was fed into the grid. As a guideline EHPs are said to reach 20 $^{kWh_{el}}/_{m^2 \cdot a}$ PV energy surplus on the average [5]. This information was used for the parameter study with ranging results of PV energy surplus between 11-64 $^{kWh_{el}}/_{m^2 \cdot a}$ for simulated EHP without battery and 6-59 $^{kWh_{el}}/_{m^2 \cdot a}$ with battery.

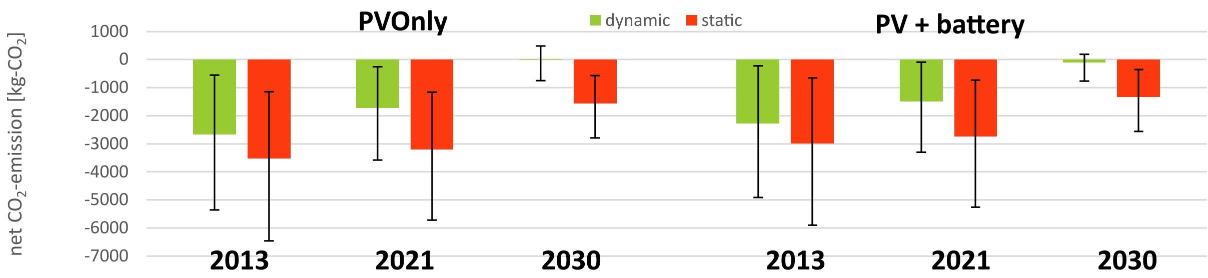

Figure 6. Comparison of calculated net CO_2 emissions for EHP in operation using the static method (red, DIN 18599) and dynamic method (green, hourly CO_2/,emission factor)

5. Critical Review

In this study we use timely resolved average CO_2 emission factors (AEF) for the German power system in order to determine the net carbon emission of an EHP. This approach implies the simplification that for each kWh_{el} additionally fed into the grid, all power plants currently online reduce their power contribution proportionally. In view of a fully functional wholesale day-ahead power market, only the marginal power plant running at the highest marginal cost is supposed to reduce its power instead. This relationship has been examined already in various studies defining the term marginal emission factor (MEF) [33, 34, 35]. Making use of the MEF requires either a fundamental model of the wholesale electricity market to identify the marginal power plant, relying on a considerable number of input data, parameters and uncertain assumptions [34], or an approximate model based on the marginal system response, which neglects must-run capacities as well as (local) transmission system restrictions [33]. Development and/or application of such a model is beyond the scope of this work. Furthermore, the MEF is determined based on a purely economic model following the merit-order. Thereby fossil fuel must-run capacities as well as (local) transmission system restrictions and measures are neglected. As a result, it remains uncertain if the marginal power plant or other, even renewable energies capacities, will be reduced in performance.

The effect of relying on AEF instead of MEF depends highly on the structure of the actual power plant fleet bidding into the respective market. With the current German power plant fleet, open cycle gas turbine often represent the marginal power plant. Their specific CO_2 emission of approx. 370 $^{g\,CO_2}/_{kWh}$ is rather in the range of the timely respective AEF in 2021 (compare **Figure 3 (c)**). That is why in this case AEF and MEF deviate only little and bring comparable results. For future scenarios with higher shares of renewable energy capacities, however, it can happen that renewable power generation pose the marginal capacities. Additionally considering fossil fueled must-run capacities, this leads to an overestimation of avoidable CO_2 emissions, especially during summertime with both approaches. We therefore highly recommend to broaden the presented methodology towards the concept of MEF. Here, MEF should be calculated with an increased level of detail regarding the mentioned points above to especially account for future scenarios with very high shares of renewable energy capacities.

6. Conclusion

In this paper the application of hourly CO_2 emission factors (dynamic method) for energy surplus single-family houses (EHP) to estimate their CO_2 emission in operation, is introduced and reviewed.

The two main findings when comparing the absolute CO_2 emissions calculated are, that, following the dynamic method, CO_2 emissions turn out to be significantly higher than those calculated with the static method. Even the case occurs, that negative CO_2 emissions are calculated with

the static method and positive CO_2 emissions are reached when using the dynamic method. The second finding relates to the comparison of EHP with and without battery. While one could expect EHP with battery to achieve lower CO_2 emissions than those without, the opposite turns out to be valid. EHP without battery show lower CO_2 emissions in operation than those with battery in 2013 and 2021, if the dynamic method is applied. In contrast, in the year 2030 EHP without battery emit slightly more CO_2 than EHP with battery.
Regarding the relative CO_2 emission factors, it can be stated, that during feed-in times of EHPs the CO_2 emission factor is significantly lower than the one during grid demand times throughout all simulated system setups. The deviation between the CO_2 emission factor of feed-in and grid power demand increases with increasing decarbonisation of the electric grid. This means that for future already partially CO_2 neutral electric power systems the avoidable CO_2 emission by PV feed-in tend to be zero since they coincide with already very high shares of renewables in the grid. Grid power demand, instead, still can be significantly CO_2 affected. This especially holds true for space heating related power demand during wintertime. Or in other words, sooner or later all EHP with a significant electricity grid demand in wintertime turn out to be net CO_2 emitters, if not the need for seasonal energy time shift is adressed.
Based on the previous findings and based on the fact that for the reviewed datasets the relative deviation of the CO_2 emission factor for feed-in and grid power demand only show very little sensitivity regarding different system setups, namely battery (non-)/existent PV capacity, electric demand, one central recommendation can be made:
The introduction of CO_2 emission factors separately for feed-in and grid use for building GHG emission evaluation within the regulatory framework seems to be highly beneficial. Both, the ISO 16745 as well as DIN 18599 already provide the possibility to consider deviating CO_2 emission factors. These new CO_2 emission factors could be determined using dynamic simulations. However, for more accurate results, the hourly AEF has to be replaced by a more specific hourly resolved CO_2 emission factor in the simulation. The emission factor has to correlate with the distinctive power plant type that is avoided in case more renewable energy is fed into the grid. Such hourly emission factor data is not available by now, as is described in the limitations. The dynamic simulation would then only need to be performed once e.g. by a public authority to determine the CO_2 emission factors applicable for any further standardized GHG emission evaluations. Before being applied on a broader basis a crosscheck whether to use AEF or MEF should be carried out carefully.

Acknowledgments

Parts of this work were developed within the research project FlexEhome: flexEhome The grid-supporting solar house with complete thermal and electric supply, funded by the German Federal Ministry for Economic Affairs and Climate Action (project reference number: 03EGB0025A). The funding is gratefully acknowledged. We would also like to thank Agora Energiewende for open data access and especially Fabian Hein regarding CO_2 emission factor calculation for future scenarios.

References

[1] United Nations Framework Convention on Climate Change 2015 Paris agreement: Fccc/cp/2015/10/add.1
[2] Bundestag 18082021 Federal climate change act (bundes-klimaschutzgesetz): Ksg
[3] Bundestag 18082021 Erstes gesetz zur änderung des bundes-klimaschutzgesetztes
[4] Röck M, Saade M R M, Balouktsi M, Rasmussen F N, Birgisdottir H, Frischknecht R, Habert G, Lützkendorf T and Passer A 2020 *Applied Energy* **258** 114107 ISSN 03062619
[5] German Federal Ministry of the Interior Building and Community What makes an efficiency house plus? principles and examples of energy-generating buildings
[6] Vuarnoz D and Jusselme T 2018 *Energy* **161** 573–582 ISSN 03605442
[7] Olkkonen V and Syri S 2016 *Journal of Cleaner Production* **126** 515–525 ISSN 09596526
[8] Lausselet C and Brattebø H 2021 *Int. J. Life Cycle Assess.* **26** 2263–2277
[9] Petra I, Thomas L and Gunter K Entwicklung der spezifischen kohlendioxid-emissionen des deutschen strommix in den jahren 1990 bis 2020
[10] Prognos, Öko-Institut and Wuppertal Institut Towards a climate-neutral germany by 2045. how germany can reach its climate targets before 2050
[11] Stein J S, Holmgren W F, Forbess J and Hansen C W 2016 Pvlib: Open source photovoltaic performance modeling functions for matlab and python *43rd Photovoltaic Specialists Conf. PVSC* ed IEEE pp 3425–30
[12] Niederl A 2017 Leistungssteigerung von photovoltaikanlagen durch modulkühlung *Innehalten und Ausblick: Effektivität und Effizienz für die Energiewende* (Verlag der Technischen Universität Graz) pp 53–54
[13] Kurz and Nawrowski 2019 *Applied Sciences* **9** 1626
[14] Wetter M and Afjei T Trnsys type 401-kompressionswärmepumpe inklusiv frost-und taktverluste
[15] Baster E 2017 *Air source heat pump modelling for dynamic building simulation tools based on standard test data* Ph.D. thesis University of Strathclyde
[16] Ralf D and Afjei Thomas e a Models of sub-components and validation for the iea shc task 44 / hpp annex 38 part c: Heat pump models
[17] Hüsing F 2020 Modelling of inverter heat pumps in trnsys *Proc. of the ISES EuroSun 2020 Conf. – 13th Int. Conf. on Solar Energy for Buildings and Industry* ed Charalambides A, Streicher W and Mugnier D (Freiburg, Germany: International Solar Energy Society) pp 1–8 ISBN 978-3-9820408-2-0
[18] Drück H Multiport store - model for trnsys: Stratified fluid storage tank with four internal heat exchangers, ten connections for direct charge and discharge and an internal electrical heater: Type 340 version 1.99f
[19] Kepplinger P, Huber G and Petrasch J 2015 *Energy and Buildings* **100** 50–55 ISSN 03787788
[20] Tjaden T April 2013 *Techno-ökonomischer Vergleich von Solarthermieanlagen mit Photovoltaik-Wärmepumpen-Systemen mittels dynamischer Simulation* Masterarbeit HTW Berlin Berlin
[21] Dipasquale C and Fedrizzi R e a Technical report on system sizing and optimised control strategies
[22] Clauß J and Georges L 2019 *Applied Energy* **255** 113847 ISSN 03062619
[23] Pollerberg C, Schmidt D L, Mönnigmann M, Löhr Y, Hörsting A, Bierwirth M, Wolf D, Kolbe C, Wiebicke C and Abul-Ella Z Schlussbericht zum verbundvorhaben: Einsatz von latentwärmespeichern mit wärmepumpen zum lastmanagement von stromnetzen - latenter stromspeicher
[24] Bundesverband Wärmepumpe eV Leitfaden hydraulik
[25] Feist W 1994 *Thermische Gebäudesimulation: Kritische Prüfung unterschiedlicher Modellansätze* 1st ed (Heidelberg: C. F. Müller) ISBN 3788074868
[26] Wystrcil D and Kalz D 2013 Model-based optimization of control strategies for low-exergy space heating systems using an environmental heat source *Proceedings of BS2013 - 13th Conf. of Intern. Building Performance Simulation Association* ed Etienne Wurtz pp 2575–2583 ISBN 9781629939988
[27] Wystrcil D and Kalz D 2014 Prädiktive regelung thermoaktiver bauteilsysteme unter berücksichtigung der hydraulischen typologie. *Human-centred building(s)* ed van Treeck C and Müller D (Aachen: RWTH Aachen University) pp 562–569 ISBN 978-3-00-047160-5
[28] Klein K, Hermann M and Herkel S 2016 *Bautechnik* **93** 1–7 ISSN 09328351
[29] Gwerder M, Lehmann B, Tödtli J, Dorer V and Renggli F 2008 *Applied Energy* **85** 565–581 ISSN 03062619
[30] Võsa K V, Ferrantelli A and Kurnitski J 2020 *Journal of Building Engineering* **31** 101387 ISSN 23527102
[31] Solar Energy Laboratory Trnsys: Volume 6 multizone building modeling with type56 and trnbuild.
[32] Glück B 1990 *Wärmeübertragung: Wärmeabgabe von Raumheizflächen und Rohren* 2nd ed Bausteine der Heizungstechnik Berechnung, Software (Berlin: Verl. für Bauwesen) ISBN 3-345-00515-8
[33] Braeuer F, Finck R and McKenna R 2020 *Journal of Cleaner Production* **266** 121588 ISSN 09596526
[34] Seckinger N and Radgen P 2021 *Energies* **14** 2527
[35] Regett A, Boing F, Conrad J, Fattler S and Kranner C 2018 Emission assessment of electricity: Mix vs. marginal power plant method *2018 15th International Conference on the European Energy Market (EEM)* (IEEE) pp 1–5 ISBN 978-1-5386-1488-4